Faraday Discussions

Accepted Manuscript

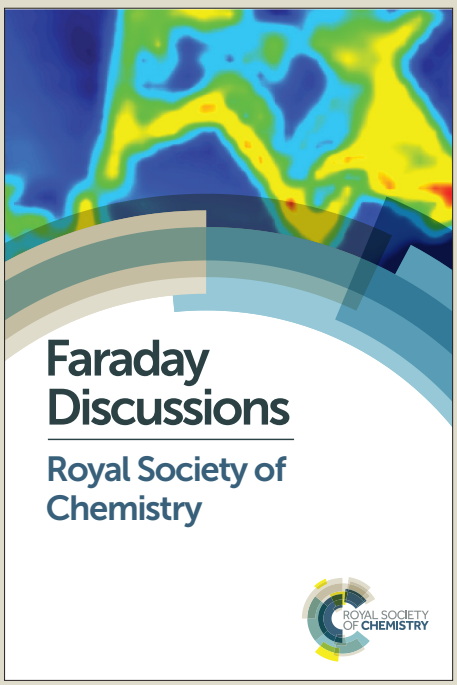

This article can be cited before page numbers have been issued, to do this please use: J. Tong, T. Hu, A. Qin, J. Z. Sun and B. Z. Tang, *Faraday Discuss.*, 2016, DOI: 10.1039/C6FD00165C.

Faraday Discussions

View Article Online
DOI: 10.1039/C6FD00165C

ARTICLE

Deciphering the Binding Behaviours of BSA Using Ionic AIE-active Fluorescent Probes

Received 00th January 20xx,
Accepted 00th January 20xx

DOI: 10.1039/x0xx00000x

www.rsc.org/

Jiaqi Tong,[a] Ting Hu,[a] Anjun Qin,[b] Jing Zhi Sun*[a] and Ben Zhong Tang*[abc]

The binding behaviors of a transport protein, bovine serum albumin (BSA), in its native, unfolding and refolding states have been probed by monitoring the emission changes of two exogenous AIE-active fluorescent probes M**2** and M**3**, which are designed to be anionic and cationic, respectively. Due to the AIE property, both of M**2** and M**3** display emission enhancement as bound to the hydrophobic cavity of BSA. The binding site of M**2** and M**3** is found to be subdomain IIA. Then, the BSA+M**2** and BSA+M**3** systems are utilized to fluorescently signal the conformation changes of BSA in various external stimuli, including thermally or chemically induced denaturation. The data confirmed the multi-step unfolding process and the existence of molten-globule intermediate state. The unfolding process undergoes the rearrangement of subdomain IIA, the exposure of a negatively charged binding site in domain I that prefers interacting with cationic species, and the transformation of molten-globule intermediate to the final random coil. The anionic and cationic modification to the probes enable us to witness that electrostatic interaction takes effect in folding and unfolding of BSA.

Introduction

Serum albumin (SA), as the most abundant circulatory protein in plasma, involves in various metabolic processes, such as determining plasma oncotic pressure, modulating fluid distribution, antagonizing activity of toxins and controlling anti-oxidant property of plasma.[1] More remarkably, SA exhibits an outstanding binding capacity for loading and transporting many endogenous and exogenous compounds.[2] In addition to the major transport protein for fatty acids,[3] SA also binds diverse metabolites, organic compounds and drugs, which make it a central role in pharmaceutics or drug pharma-cokinetics.[4] SA helps with dissolution of hydrophobic compounds, distribution of ligands through the whole body, and resistance of these ligands to being metabolized.[5] Bovine serum albumin (BSA), a kind of homologous protein of serum albumin, consists of 583 amino acid residues and forms a single polypeptide chain. BSA adopts a heart-shaped structure, constructed by about 67 % α-helix and seventeen disulphide bridge, and it is divided into three homologous domains I, II and III, which are further partitioned into two subdomains A and B (Figure S1).[6] As a typical SA, BSA is an area of current intense research, since it is a reference to the study of SA or human serum albumin (HSA) and can be used as a model for understanding basic principles of protein issues. Reasonably, elucidating properties of BSA can help us in better understanding of HSA properties and designing new albumins with improved functionality, which can even be used as a deputy of HSA.[7] Moreover, not only are the various binding aspects of serum albumins concerned, but also the conformational dynamics of the protein towards diverse stimuli are followed, since it is conducive to control efficiently delivery of drugs and, more importantly, deeply understand functional principles of protein at molecular level.[8]

A number of works dealing with binding of sundry ligands to BSA/HSA have been reported by using techniques such as circular dichroism spectroscopy, nuclear magnetic resonance, fluorescent spectroscopy and so forth.[9,10] Among them, fluorescent spectroscopy is widely applied, based on the intrinsic fluorescence from BSA or the extrinsic fluorescence from a variety of binding fluorogens.[10] The fluorogens displaying changes in emission features (intensity, wavelength and/or lifetime) can be used to signal the binding process of themselves to BSA and act as non-covalent labels of BSA. Through the detectable feature changes, the information about the binding aspects of BSA has been successfully collected in a certain detail. However, the studies based on fluorescent probes are still limited because of the lack of well-performed fluorogens or dyes. For example, there exists a problem

[a] *Dr. Jiaqi Tong, Ms Ting Hu, Prof. Jing Zhi Sun, Prof. Ben Zhong Tang*
MoE Key Laboratory of Macromolecular Synthesis and Functionalization
Department of Polymer Science and Engineering
Zhejiang University, Hangzhou 310027, China
E-mail: sunjz@zju.edu.cn.
[b] *Prof. Anjun Qin, Prof. Ben Zhong Tang*
Guangdong Innovative Research Team
State Key Laboratory of Luminescent Materials and Devices
South China University of Technology, Guangzhou 510640, China.
[c] *Prof. Ben Zhong Tang*
Division of Biomedical Engineering, Department of Chemistry, Hong Kong Branch of Chinese National Engineering Research Center for Tissue Restoration and Reconstruction, Institute for Advanced Study, Division of Life Science, Institute of Molecular Functional Materials and State Key Laboratory of Molecular Neuroscience, The Hong Kong University of Science & Technology (HKUST), Clear Water Bay, Kowloon, Hong Kong, China
E-mail: tangbenz@ust.hk.

† Footnotes relating to the title and/or authors should appear here.
Electronic Supplementary Information (ESI) available: [Conformational structure of BSA in its native state, fluorescence spectra for the mixtures of BSA and M**2**/M**3** in different conditions.]. See DOI: 10.1039/x0xx00000x

that some dyes emit less efficiently when binding to the pockets or cavities of proteins than dispersing in aqueous media.[11] Some others change their emission colors when they bind to the target proteins. Normally, this kind of fluorescent probes show blue-shifted emission band in the hydrophobic pockets of the binding proteins, in comparison with the more hydrophilic environment before binding. As a result, the environment-sensitive fluorescent probes offer a unique colorimetric method to signal the binding process.

In 2006, a new kind of fluorescent probes with aggregation-induced emission (AIE) property was reported to be used in the fluorescent detection of BSA.[12] In a typical AIE process, the weakly emissive fluorogens are induced to emit strongly by the formation of aggregates. The mechanistic studies revealed that the restriction of intramolecular motion (RIM) processes account for the AIE phenomenon. So far, the RIM processes can be mainly classified into two specific situations, which are the restricted intramolecular rotations (RIR) and restricted intramolecular vibrations (RIV) for propeller- and shell-like luminogen systems, respectively.[13] As shown in Chart 1, the first reported AIE-active luminogen or AIE-gen used in BSA detection is a tetraphenylethene (TPE) derivative (M**1**).[12] Due to the two quaternary ammonium cations, M**1** is soluble in aqueous buffer solutions and shows faint fluorescence. But the TPE core is intrinsically hydrophobic. Once the probe molecules are engulfed by the hydrophobic pockets of BSA or HSA, the RIM effect of the propeller-shaped TPE luminogen takes on and the molecules become highly fluorescent. According to the AIE mechanism, BSA or HSA is detected by reading the variation of the fluorescence intensity.

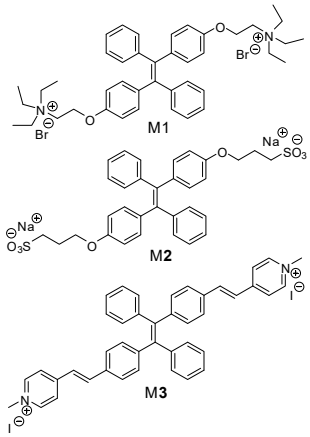

Chart 1. Chemical structure of the AIE-active fluorescent probes.

The molecular design was renewed by H. Tong *et al.* through replacing the two quaternary ammonium cations with two sulphonate anions (M**2**, Chart 1),[14] because the sensitivity of M**1** in the detection of protein was undesirable. BSA could be detected at a concentration as low as 500 ng/mL by using M**2** as a fluorescent probe. The calibration curve exhibited a quite wide linear range (0~100 μg/mL). A significant observation was that the fluorescence of M**2** could not be turned on by denatured BSA. Thus the fluorescence enhancement in the existence of BSA was rationally associated with the binding of M**2** to the hydrophobic pockets within BSA, which disappeared in the denatured state. Based on this detection mechanism, it was envisioned that even lower BSA level could be detectable at higher M**2** concentration without suffering from the self-quenching problem of traditional organic dyes. By introducing TPE moieties into the side chains of a water soluble polymer, the detection sensitivity to BSA was further boosted up to an ultra-high level of 0~0.6 ppm.[15]

Besides the unique detection mechanism and high sensitivity, the BSA detection with AIE-active probe M**2** showed other advantages. For example, the detection is not interfered by the presence of different bioelectrolytes in artificial urine. Thus the methodology is put to use in the investigations on different processes of proteins, such as the visualization of the hydrophobic pockets of proteins and catalytic sites of enzymes, the monitoring of the conformational changes and amyloid fibrillation process, and the specific binding of cyclic arginine-glycine-aspartic acid (cRGD) towards integrin $\alpha_v\beta_3$.[16] The study on the conformational transitions of human serum albumin (HSA) was also tried.[17] The weakly emissive M**2** in buffer solution became strongly emissive upon the addition of native HSA, but the emission could not be triggered out by HAS in the presence of guanidine. Combining the RIR and Forster resonance energy transfer mechanism, the unfolding process of HSA was elucidated in unprecedented details.[17] With increasing the concentration of the denature agent of guanidine hydrochloride (GndHCl), the native HSA underwent a multi-step transition process involving domain separation, molten globule and finally unfolded coil.

Despite these substantial progresses, further understanding of the BSA-ligand binding process and the conformational transitions between native and denatured states is still of great scientific significance. For example, both dicationic and dianionic AIE-active fluorogens (M**1** and M**2**) had been used in the previous works, and they clearly showed fluorescent responses to BSA binding. Given that BSA is a transportation protein possessing different pockets, do the cationic and anionic probes bind to the same hydrophobic pocket of BSA? If yes, can we conclude that the binding of fluorogens to BSA depends solely on the hydrophobic effect? If not, what is the role of the charged groups playing in the binding process? Furthermore, it is assumed that some proteins undergo a hysteresis loop of folding→unfolding→refolding process. Can we acquire further understanding of the folding→unfolding→refolding behaviours of BSA?

In the hope of getting further understanding of the above issues, two TPE-derivatives are used to study the detailed processes of the interest in this work and their structures (M**2** and M**3**) are shown in Chart 1. M**2** is used in the present work for its excellent sensitivity to fluorescently response BSA as reported in literature.[14] The reason for the choice of M**3** is based on two considerations: (1) In previous work, it was noted that the cationic M**1** had lower sensitivity than the anionic M**2**.[14,15] The difference in sensitivity may be associated with the difference in the size of the charged species. For M**1**, the positive charge localizes inside the bulky triethylbutyl-ammonium. According to Coulomb's law, the strength of electrostatic attraction follows the inverse square law, the bulky size of triethylbutylammonium would weaken the Coulomb's force thereby results in the lower sensitivity. For M**3**, the pyridinium cation has a smaller size than the triethylbutyl-ammonium moiety

and it exposes directly to its surrounding. We thus expect M**3** will display higher sensitivity than M**1**. (2) M**1** and M**2** emit identical fluorescence because they have the same luminogen, although they bear opposite static charges. M**3** is composed of a TPE core and two pyridinium moieties. The C=C double-bond linkage expands the effective conjugation hence allows M**3** to emit red-shifted fluorescence. The difference in emission color benefits the examination of relevant processes using M**2** and M**3** concomitantly.

Experimental Section

Chemicals. The synthetic routes to the anionic and cationic TPE derivatives (M**2** and M**3**) and their AIE behaviors were reported elsewhere.[14,18] Unless otherwise noted, all reagents were purchased from commercial suppliers and used without further purification. The purchased BSA was further purified according to literature[19] so as to make the protein free of fatty acids. Routine phosphate buffer (containing 10 mM Na_2HPO_4, 2 mM KH_2PO_4, 137 mM NaCl and 2.7 mM KCl) was prepared by dissolving corresponding components in deionized water and adjusting pH to a final value of 7.40. Phosphate buffers used for study influences of pH on folding of BSA were prepared by mixing certain amounts of H_3PO_4, NaH_2PO_4 or Na_2HPO_4 in deionized water and adjusting pH to specified values with NaOH or HCl. Stock solutions of M**2** and M**3** were prepared by dissolving appropriate amounts of the two probes in the aqueous phosphate buffer to a concentration of 20 μM. The stock solution of BSA (20 μM) in phosphate buffer was prepared based on its molecular weight of 66.4 kDa and the concentration was further checked by measuring absorbance at 280 nm with an extinction coefficient of 44720 $M^{-1}\cdot cm^{-1}$.[14]

Measurements. For fluorescence (FL) titration, aliquots of a BSA solution were added to 1 mL of an M**2** or M**3** solution, which was then diluted with the phosphate buffer to a final volume of 10 mL. For energy transfer experiments, BSA concentration was fixed at 1 μM while a set of the dye solutions with increasing amounts were added and finally diluted to the concentration of 0~10 μM. For thermal denaturation, the concentration of the probes and BSA were kept at 1 μM, and the samples were incubated at designed constant temperature for 10 min before taking the measurements through an accessional water bath. For the unfolding experiments caused by urea or guanidine hydrochloride, a series of diluted solutions of the denaturants with varied concentrations were sequentially mixed with certain amount of BSA and a probe, both of which have a final constant concentration of 1 μM. For pH-induced unfolding, BSA and the probes were firstly mixed with phosphates (H_3PO_4, NaH_2PO_4 or Na_2HPO_4) in deionized water and then pH of the solutions was adjusted to specified values with NaOH or HCl. Except thermal denaturation experiments, all the samples were incubated for 30 min to achieve equilibrium prior to measurements and all the measurements were carried out at ambient temperature (~25 °C). FL spectra were recorded on a spectrofluorophotometer of Shimadzu RF-5301PC. UV-vis absorption spectra were recorded on a Varian VARY 100 Bio UV-vis spectrophotometer

Results and Discussion

Confirmation of the binding of M2 and M3 to BSA.

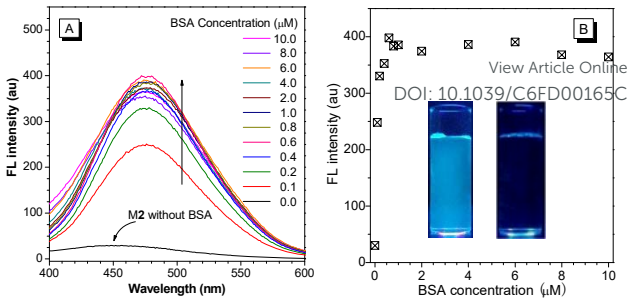

Figure 1. (A) Fluorescence (FL) spectra of M**2** in aqueous phosphate buffer solutions (pH 7.4) with different concentration of BSA. (B) Variation of FL peak intensity with BSA concentration, in which the data are extracted from spectra shown in (A) at emission wavelength of 459 nm for the sample without BSA and 476 nm for other samples. Excitation wavelength (λ_{ex}): 330 nm; M**2** concentration ([M**2**]): 1 μM. Inset of (B): Photographs showing the emission of M**2** in buffer solutions (pH 7.4) with and without BSA taken under illumination with 365 nm UV-light.

The binding of M**2** to BSA had been reported in the previous work.[14] To keep the experimental conditions consistent in the present work, we set the pH value of the phosphate buffer solution at 7.4 as the common condition, which was composed of 10 mM Na_2HPO_4, 2 mM KH_2PO_4, 137 mM NaCl, 2.7 mM KCl and deionized water. The emission behaviour of M**2** (1.0 μM) was examined in aqueous phosphate buffer solutions (pH 7.4) with different concentrations of BSA (referred as BSA+M**2** system below). As shown in Figure 1A and 1B, M**2** emits weakly in the buffer solution and the emission peak appears at 459 nm. After addition BSA into the buffer solution containing 1.0 μM of M**2**, the emission intensity is immediately boosted up and the emission peak red-shifts to around 476 nm. The changes of FL intensity can be intuitively revealed by the photographs of the inset of Figure 1B, which shows the obviously enhanced greenish-blue emission from the buffer solution containing BSA. Quantitatively, the FL intensity recorded for the system containing 0.1 μM of BSA increases to about 10 times of that recorded for the absence of BSA. When BSA concentration increases to about 0.6 μM, the emission achieves the saturation intensity, and about 12-fold enhancement was recorded. These characteristics are in good agreement with the results reported in previous works,[14] indicating that the changes in FL features are convincing messages to signal the binding between BSA and M**2**.

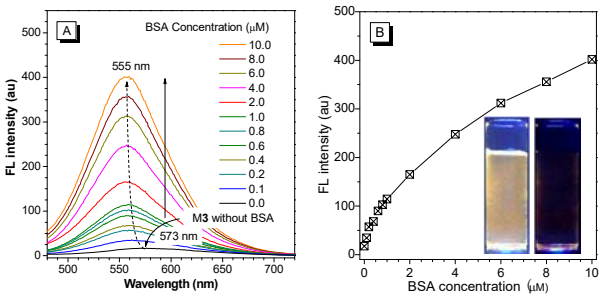

Figure 2. (A) FL spectra of M**3** in aqueous phosphate buffer solutions (pH 7.4) with different concentration of BSA. (B) Variation of FL peak intensity with BSA concentration, in which the data are extracted from spectra shown in (A). Excitation wavelength (λ_{ex}): 395 nm; [M**3**] = 1 μM. Inset of (B): Photographs showing the emission of M**3** in buffer solutions (pH 7.4) with and without BSA taken under illumination with 365 nm UV-light.

Under the same experimental condition, the variation of the emission features of M**3** (1 μM) upon addition different concentrations of BSA (referred as BSA+M**3** system in below) are demonstrated in Figure 2A and 2B. The general trends of emission feature are similar to those observed in BSA+M**2** system. M**3** is faintly emissive in buffer solution in the absence of BSA. Increasing the concentration of BSA, FL intensity grows stronger and stronger. According to the RIR mechanism and the understanding derived from our previous works, M**3** can also be used as a fluorescent reporter of BSA-probe interaction. But the details of the emission features of BSA+M**3** system demonstrate some differences from BSA+M**2** system.

Firstly, the emission peak of M**3** in the phosphate buffer solution appears at around 573 nm, indicating an orange emission. The wavelength gap between M**2** and M**3** is nearly 100 nm, which can be easily recognized by their emission colors and thus helpful to be used simultaneously in the comparative study of BSA-binding events. Meanwhile, the emission intensity of BSA+M**3** system is comparative to that of BSA+M**2** when the concentration of BSA is 4.0 M, indicating that M**3** is better than M**1**. Secondly, when adding BSA to the M**3**-containing solution, the emission peak appears at around 555 nm, indicating a blue-shift of 18 nm (573 to 555 nm). This is distinct from those observed for BSA+M**1** and BSA+M**2** systems. The fluorophore of both M**1** and M**2** is TPE moiety with two electron donating alkyloxyl groups, but the fluorophore of M**3** is not a TPE moiety but an extended conjugation system with two pyridinium moieties conjugating with the TPE core. Because of the enlarged molecular size of M**3**, we tentatively infer that the conformation of M**3** should be more twisted when it binds to BSA in order to be accommodated by the hydrophobic pocket. Thirdly, comparing the plots in Figures 1B and 2B will find that the emission intensity of BSA+M**3** system enhances gradually with the increase of BSA concentration, but for BSA+M**2** system the emission intensity grows steeply with the addition of BSA. The difference implies the interaction mode between BSA and M**2** may be distinct from BSA and M**3**.

Estimation of binding constants of M2 and M3 to BSA.

The emission enhancement of the M**2** and M**3** in the presence of BSA have disclosed some information about the binding of the probes to BSA, but the detailed binding mechanisms such as binding constant and binding sites need to be further and carefully explored. To elucidate these issues, the principle of fluorescence resonance energy transfer between BSA and M**2** or M**3** is adopted. BSA has three fluorophores, which are tryptophan (Trp), tyrosine (Tyr) and phenylalanine (Phe). The intrinsic fluorescence of BSA is mainly attributed to the Trp residue, because of the particular weak fluorescence of Phe and the nearly totally quenched fluorescence of Tyr residue. BSA contains two Trp residues, i.e. Trp-134 and Trp-212, locating in IB and IIA subdomains, respectively (Figure S1).[20] According to theory of Förster's resonance energy transfer (FRET), efficient energy transfer generates if there exists a certain degree of spectral overlap between the emission band of the donor and the absorption band of the acceptor and meanwhile the distance between the donor and acceptor is within 2~8 nm. Based on the FRET principle, the emission intensity of the donor and acceptor would gradually decrease and increase respectively, as the concentration of the acceptor increases.[21]

The changes in the intrinsic fluorescence of BSA with adding increasing amount of M**2** or M**3** have been measured and the recorded data are depicted in Figures 3 and S2. The FL spectrum of the native BSA displays a single band with the peak at 345 nm. After a certain concentration of M**2** or M**3** was mixed with BSA, the FL from BSA became weaker. Quenching of the BSA's fluorescence by adding M**2** or M**3** is associated with the energy transfer from the protein's fluorophores to M**2** or M**3**. In order to quantitatively evaluate the protein-probe interactions, the quenching data of BSA fluorescence were examined by the Sterm-Volmer equation:[22]

$$\frac{F_0}{F} = 1 + K_{sv}[Q] \quad (1)$$

Where, F_0 and F are the emission intensities of the fluorophore (Tyr in BSA) in the absence and presence of the quencher (M**2** or M**3**); [Q] and K_{sv} stand for the quencher concentration and the Stern-Volmer quenching constant, respectively. Based on equation (1), the binding constant and the binding affinity of the probes to BSA can be further estimated with a modified version of the Stern-Volmer equation which is given by:

$$\log\frac{F_0 - F}{F} = \log K + n\log[Q] \quad (2)$$

Where K and n are the binding constant and the number of the binding site, respectively. According to equation (2), the plot of $\log[(F_0\text{-}F)/F]$ versus $\log[Q]$ is calculated and shown in Figure 3B. For the complex BSA+M**2**, the calculated values of the binding constant (K) and the number of binding sites (n) are 5.50×10^7 L/mol and 1.42, respectively. For the complex BSA+M**3**, the K and n value is turned

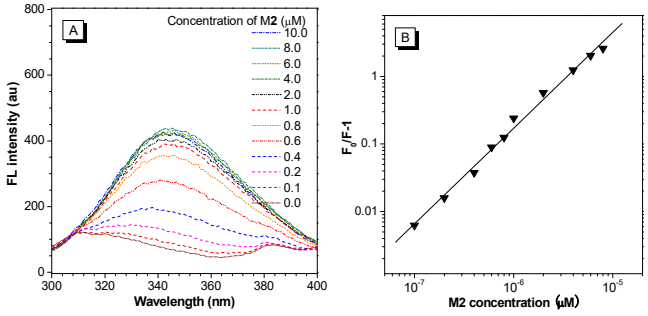

Figure 3. (A) Fluorescence (FL) spectra of BSA in the presence of different [M**2**]. (B) Plot of lg [(F_0-F)/F] vs. lg [M**2**]; F_0 and F: the peak FL intensity of BSA without M**2** and with different [M**2**] values. BSA concentration: 1 μM; λ_{ex}: 280 nm.

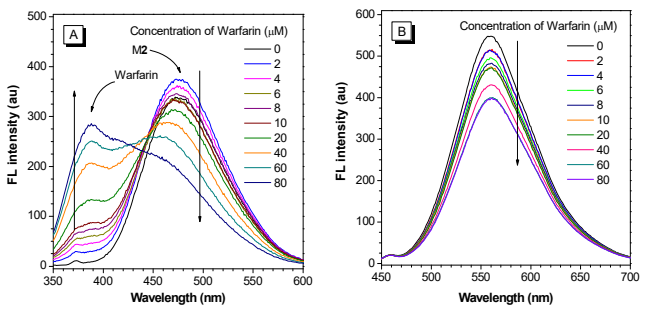

Figure 4. (A) FL spectra of BSA+M**2** system in the presence of warfarin, λ_{ex}: 330 nm, Concentration of BSA: 1 μM. (B) FL spectra of BSA+M**3** system in the presence of warfarin, λ_{ex}: 395 nm. Concentration of warfarin: 0~80 μM; concentration of BSA: 1 μM; concentration of M**2** or M**3**: 5 μM.

to be 1.38×10^6 L/mol and 1.21, respectively (Figure S2). The numerical values of *n* indicate that only one biding site in native BSA is involved with the binding of M**2** or M**3**.

Estimation of binding sites of M2 and M3 to BSA.

Based on the above data, the exact binding sites of the two probes in BSA can be further checked. The two fluorophores, Trp-134 and Trp-212 are locating in sub-domain IB and IIA, respectively. Accordingly, the probes are likely to bind to the sub-domains IB and IIA. In other words, domains bound by M**2** or M**3** are approximate to where the fluorophores localize, since no fluorescence quenching is expected to occur if the probes bind to the sites that are far away from Trp-134 or Trp-212.

Besides FRET strategy, the replacing effect of various known site-selective binding ligands on the binding of M**2** or M**3** was examined to help understanding of the binding process. If the ligand binds to the same region as the probes in BSA, the ligand has a competitive effect or an inhibitory effect on the interaction of M**2** or M**3** and BSA. Namely, adding the ligand to the BSA-M**2** or BSA-M**3** complex can cause exchange between the ligand and the probe molecules thereby gradual decrease of fluorescence intensity. Based on this idea, the effect of ligand addition on the interaction of M**2** and BSA was studied. Previous works reported that there are more than one binding sites for fatty acids in BSA with different extents of affinity to the ligands.[23] It has been confirmed that BSA has three high affinity sites or three primary binding sites to myristic acid (a fatty acid), which consist of one site in subdomain IIIA, one in subdomain IIIB and one at the interface between subdomain IA and IIA. The change in fluorescence intensity of M**2** in BSA solutions which had been incubated with growing amounts of myristic acid was monitored (Figure S3). The obtained results demonstrated that almost no change in the emission intensity of M**2** had occurred. This observation indicated there was no exchange between myristic acid and M**2** molecules, therefore it can be inferred that M**2** binds to a site (or some sites) different from the binding sites specifically for myristic acid. Therefore, it can be concluded that the binding event of BSA to M**2** has not occurred at the high affinity sites of BSA to myristic acid (subdomain IIIA, subdomain IIIB and the interface between subdomain IA and IIA). Similar experiments have been carried out to BSA+M**3** system. Due to the electrostatic interaction between M**3** and myristic acid, the mixture of M**3** and myristic acid showed emission enhancement when the concentration of myristic acid was increased to a certain threshold (~ 6×10^{-6} mol/L) (Figure S4A and S4C). In the presence of BSA, M**3** probe is mostly encapsulated in certain hydrophobic domain of BSA, and this domain must have weak binding capacity to myristic acid. As a result, M**3** are seldom replaced by myristic acid molecules and the electrostatic interaction with myristic acid molecules becomes much weaker. Therefore, the emission behaviour of M**3**+myristic acid in the presence of BSA (Figure S4B) is different from that observed in the case of the absence of BSA, but similar to that displayed in Figure S3. According to these results, we can conclude that the binding of M**3** to BSA does not occur at the same sites of myristic acid, i.e. the sites of subdomain IIIA, subdomain IIIB, the interface between subdomain IA and IIA.

Then the two principal drug-binding sites, subdomains IIA and IIIA were checked, which were reported by pioneering work of Sudlow and thereby named as Sudlow I and II.[24] Since the above-mentioned data have shown that Sudlow II is hardly a binding site of M**2** and M**3**, the displacing effect of site-selective binding ligands for Sudlow I, such as warfarin, on the binding of M**2** and M**3** was investigated. After adding warfarin to the solution of BSA-M**2** complex, gradual decrease of the fluorescent intensity corresponding to M**2** at 475 nm is observed. This process is accompanied with an emission enhancement of warfarin (Figure 4A). A similar effective displacement in the case of warfarin and BSA-M**3** complex has also been found (Figure 4B). According to the RIM mechanism of AIE-activity, the decrease of FL intensity of M**2** and M**3** can be ascribed to the releasing of M**2** and M**3** from the binding site of BSA, which emancipates the movement restriction of the fluorogens in the binding state. This releasing is obviously caused by the displacement of M**2** and M**3** with warfarin. Thus, it is concluded that the two probes, both M**2** and M**3**, are bound to the Sudlow I or subdomain IIA of BSA, which is a principal drug-binding site.

Thermal denaturation of BSA signaled using M2 and M3 as extrinsic fluorescent probes.

According to the derived results, the negatively charged probe M**2** and positively charged probe M**3** show identical binding performance to BSA in native state. It seems that the binding event only correlates with the hydrophobic effect of the binding site but is regardless to the electrostatic interaction. In fact, electrostatic interaction plays crucial roles in many protein-related biological processes. It has been well-accepted that the information about the binding proteins to the ligands can be inferred from their denaturation processes. As one of the characteristic properties of proteins, thermal denaturation may causes the native protein structure to be disrupted and lose the functional conformation.[25] A comprehensive study of the thermal stability of proteins (including BSA) will be conducive to understand the biological regulation and function mechanisms of the proteins responding to stimuli of internal and external environment. By dint of the fluorescent characteristics of the two probes when bound to BSA discussed above, we detected the structure changes and the ligand-binding properties of BSA in the unfolding and refolding processes impacted by temperature rising and falling.

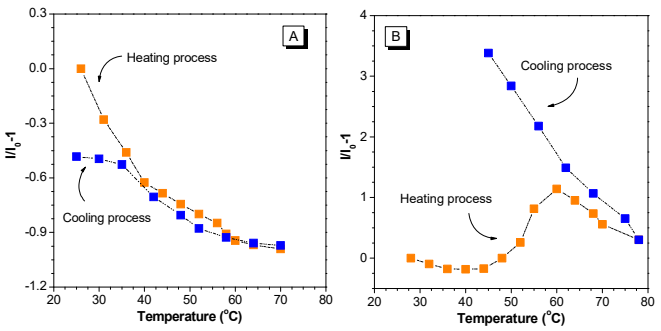

Figure 5. Plots of the relative fluorescent intensities (I/I_0) of (A) BSA+M**2** and (B) BSA+M**3** system in PBS buffer (pH=7.4) as a function of temperature in the heating (from 25 °C to 75 °C, orange) and the following cooling processes (from 75 °C to 25 °C, blue). I_0 and I: the peak FL intensity of the system at 25 °C and at different temperatures. λ_{ex}: 330 nm for M**2** and 395 nm for M**3**; Concentration of M**2** and M**3**: 1 μM; Concentration of BSA: 1 μM.

The peak emission intensity and emission spectra of BSA+M**2** at different temperatures ranging from 25 °C to 70 °C are displayed in Figure 5A and S5. A monotonous reduction of the emission intensity was observed with the elevation of temperature. When it comes to the system of BSA+M**3** (Figures 5B and S6), an initial diminution of fluorescent intensity, which is similar to the case of BSA+M**2** is followed by a palpable enhancement of the intensity as the temperature reached over 45 °C. Then the intensity goes through a subsequent decrease when the temperature increases to 60 °C or above. Given the fact that the fluorescence intensity of the two AIE-active probes has a decrease themselves as temperature rises up, the attenuation of the emission intensity of the two complexes cannot be directly and fully attributed to the structure change of the binding site. However, the dissimilar enhancement in the case of BSA-M**3** indicated that there does exist an intermediate state at around 50 °C, which has something to do only with probe M**3**.

The refolding processes of BSA in the two systems with lowering the temperature from 70 °C to room temperature were then recorded based on the conversions of emission properties (Figure 5B). As the BSA+M**2** system was cooled from 70 °C to ambient temperature, the fluorescent intensity ascended, though it did not return to the original intensity before the heating-cooling cycle. It implies that the structure of BSA may have not completely transformed to its original conformation but a conformation that is different from the native one, which has low binding capacity to M**2** molecules. In the cooling process, the fluorescence of BSA+M**3** system enhanced steeply and monotonously, and the intensity was evidently higher than the original state (Figure 5B, blue squares). These spectral changes indicate that the BSA refolding process in the cooling run dose not compile the unfolding process by heating. The refolded BSA has a new intermediate conformation that has special domain(s) to accommodate more M**3** molecules or has stronger ability to restrict the intramolecular rotations or vibrations of M**3** when temperature went down from 70 °C to 25 °C.

The "abnormal" fluorescent responses of BSA+M**3** system in the cooling process may be caused by a certain possible damage to BSA at 70 °C.[26] In order to get rid of this possibility, we repeated the heating-cooling cycles by a procedure of heating the systems to 50 °C and subsequently cooling the system to room temperature. The emission behavior of BSA+M**2** was quite similar to that shown in Figures 6A and S7. The FL intensity of M**2** underwent a diminution in the heating process and largely recovered to its inception in the cooling process. In heating process, the emission intensity of M**3** exhibited a monotonous decrease before 42 °C. But an evident emission enhancement was recorded as the temperature reached to about 45 °C and higher. In the cooling process, a distinct and durative enhancement of emission was observed (Figures 6B and S8). Based on these data, it is reckoned that there exists a domain in the intermediate state (around 45 °C) that is able to effectively bind with M**3**. This domain may be buried in the native state of BSA thus it is inaccessible to be bound by M**3**. When BSA converted to the intermediate state upon temperature rising, the domain exposes to the outside and it becomes accessible.

The reversible and irreversible structural alterations of BSA were previously described on the basis of a two-step model.[27] It was reported that increasing temperature to around 50 °C led to a reversible separation of domains I and II; and heating to a higher temperature of 70 °C led to irreversible unfolding (denaturation) of domain I and II.[27] At room temperature, both M**2** and M**3** bind to the same subdomain IIA of BSA in the native state, though they bear ion groups with opposite charges. The subdomain IIA will go through an irreversible damage when the temperature exceeds 70 °C. When the conformation of the albumin reversibly adjust to an intermediate state through changing the temperature to 50 °C, the already existing binding site, which selectively interacts with M**3** containing cationic group, start to function and combine with M**3**. It is inferred that the positive charged M**3** binds to domain I of BSA in the intermediate state since domain I, which has strong negative charge, can serve as a suitable binding site for cationic probes.[28]

Unfolding induced by guanidine hydrochloride and urea.

The different responses of M**2** and M**3** to the temperature-induced unfolding and refolding processes of BSA suggest the ligand binding behaviours of BSA really have something to do with electrostatic interaction between the host and guest. In order to get further understanding of these processes, a study on the chemical denaturation of BSA induced by guanidine hydrochloride (GndHCl) was carried out by monitoring the variations of fluorescent spectral features of M**2** and M**3** in the presence of BSA, since it has been shown that some chemicals including GndHCl can cause BSA unfolding.[29] Figures 7, S9 and S10 display the plots of emission

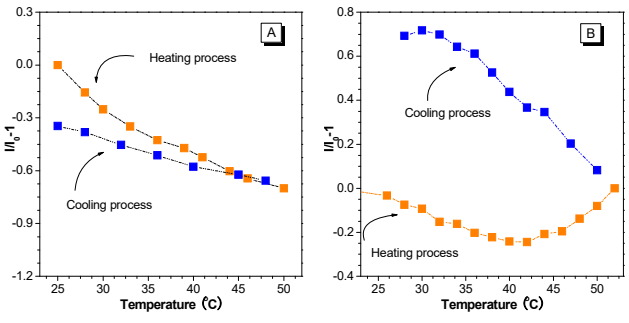

Figure 6. Plots of the relative fluorescent intensities (I/I_0) of (A) BSA+M**2** and (B) BSA+M**3** systems in PBS buffer (pH=7.4) as a function of temperature in the heating (from 25 °C to 52 °C, orange) and the following cooling processes (from 52 °C to 25 °C, blue). I_0 and I: the peak FL intensity of the system at 25 °C and at a different temperature. λ_{ex}: 330 nm for M**2** and 395 nm for M**3**; Concentration of M**2** and M**3**: 1 μM; Concentration of BSA: 1 μM.

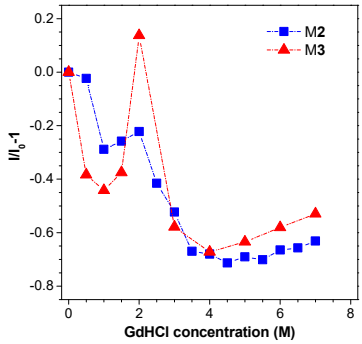

Figure 7. Effect of GndHCl on the relative FL intensity (I/I_0) of M**2** and M**3** in the presence of BSA in PBS buffer (pH = 7.4). I_0 and I: the peak FL intensity of the sample without GndHCl and with different concentrations of GndHCl. λ_{ex}: 330 nm for M**2** and 395 nm for M**3**. Concentration of M**2** and M**3**: 1 μM; Concentration of BSA: 1 μM.

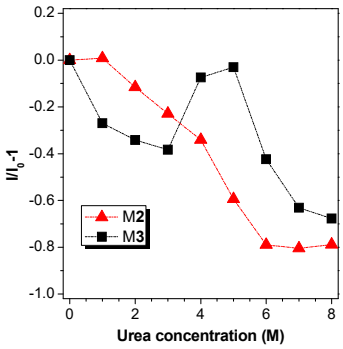

Figure 8. Effect of urea concentration on the FL intensities (I/I_0) of M**2** or M**3** with BSA in PBS buffer (pH = 7.4). I_0 and I: the peak FL intensity of the sample without urea and with different concentrations of urea. λ_{ex}: 330 nm for M**2** and 395 nm for M**3**. Concentration of M**2** or M**3**: 1 μM; Concentration of BSA: 1 μM.

maxima of M**2** and M**3** in BSA buffer solution together with GndHCl in different concentrations. As a whole, the emission intensity becomes weaker and weaker along with gradual increase of the denaturant amount. This trend suggests the probe molecules are released from the hydrophobic pockets of BSA due to the denaturation induced by GndHCl, which can be mainly ascribed to the structural loss of subdomain IIA.

In details, several turning points have been revealed in the plots. As shown in Figure 6, the peak fluorescence intensity displays a transition step at GndHCl concentration of 1.0 M for both of M**2** and M**3**. Before this GndHCl concentration, the peak fluorescence intensity drops monotonously. Afterwards, fluorescence intensity begins to boost up and reaches to its crest at around a GndHCl concentration of 2.0 M, which is followed by a secondary intensity decrease. When GndHCl concentration increases to about 4.0 M, the fluorescence of the system demonstrates small enhancement. The significant fluorescence enhancement at a GndHCl concentration of 2.0 M can be associated with the formation of a favorable rearrangement of subdomain IIA or a wider domain involving domains I and II. Such intermediates increase in the binding of the probe molecules to the transformed BSA. A similar transition behavior was observed for HAS+M**2** system and it was explained by the formation of molten-globule intermediate,[17] which can provide larger or more hydrophobic regions to bind the probe molecules and thereby induce stronger emission.

To further validate the mutual existence of hydrophobic and electrostatic interactions in the target binding events occurring to BSA in different states, we examined the fluorescent responses of BSA+M**2** and BSA+M**3** systems in the presence of urea. As shown in Figure 8, for BSA+M**2** system, the FL intensity goes down monotonously with the increase of urea concentration and levels off when urea concentration reaches and exceeds 6 M (see also Figures S11 and S12). But for BSA+M**3** system, the FL intensity decreases in the urea concentration range of 1.0 ~ 3.0 M, and a sharp emission enhancement can be observed in the urea concentration range of 4.0~5.0 M. Finally, the emission intensity declines when the urea concentration is higher than 6.0 M.

Obviously, these data demonstrate different responses of BSA+M**2** and BSA+M**3** systems to GndHCl and urea. We tentatively associate the differences with the distinct denaturation effects on proteins between urea and GndHCl. Generally, GndHCl and urea have the structural similarity, and both of them can denature or unfold proteins through hydrogen-bonding interaction between the N-H moiety of urea and the carbonyl oxygen part of the protein backbone. As a charged denaturant, besides the hydrogen bonding effect, GndHCl would interact with the oppositely charged residues in protein through electrostatic force, which helps the protein unfolding process.[30] According to literature, the intermediates with urea and GndHCl are similar to each other with a denatured domain III and rearrangement of domains I and II. In the presence of around 1.0 M GndHCl, BSA attains a state with rearrangement and separation of domains I and II.[31] These conformational changes may lead to the releasing of partial encapsulated probe molecules into the buffer solution and the reduction of FL intensity. At around 1.5~2.0 M GndHCl, the depriving of water molecules from BSA surface results in the exposure of the hydrophobic residual sequences to the environment, thereby the probe molecules of M**2** and M**3** find cavities to bind on partially denatured BSA, which may possess a molten-globe state. Consequently, an increment of FL intensity has been observed in Figure 7A and 7B at this GndHCl concentration range. The rearrangement of domain IA uncovers the negatively charged residues like Asp, which helps the binding of positively charged M**3** to the hydrophobic molten-globe intermediate, thus the BSA+M**3** system shows higher FL intensity than BSA+M**2** system. Further addition GndHCl into the two systems causes the sharp decrease in FL intensity. At higher GndHCl concentration (e. g. > 2M), BSA is largely denatured and loses its native structure and becomes random coil thus forfeits the original binding ability to M**2** and M**3**.

Without net charge, urea shows weaker denaturation ability than GndHCl. It needs higher concentration of urea to unfold BSA. As reported in literature, the state in the presence of ~ 4.5 M urea keeps a partial loss of the native form of domain I along with the unfolding of domain II.[32] In this stage, the original pocket is totally deformed and the bonded M**2** or M**3** molecule sets free to the buffer solution. As a result, the FL intensity evidently declines (Figure 8). At the same time, the deformation of domain I liberates Asp residues, and this form exhibits a strong affinity to positively charged M**3** probes, which induces the enhancement of FL intensity of M**3** in the presence of over 4.5 M urea. This behavior has not been observed in the case of GndHCl, because GndHCl is a denaturant with positive charge, which effectively shields the electrostatic interaction between cationic M**3** and the negatively charged net of the deformed domain I.

The above results and discussion indicate that electrostatic interaction between the probe and deformed BSA plays a crucial role in the denaturing process. To offer further proof, we then examined the effect of pH, especially under acidic condition, on the structural change of BSA by monitoring the fluorescent features of

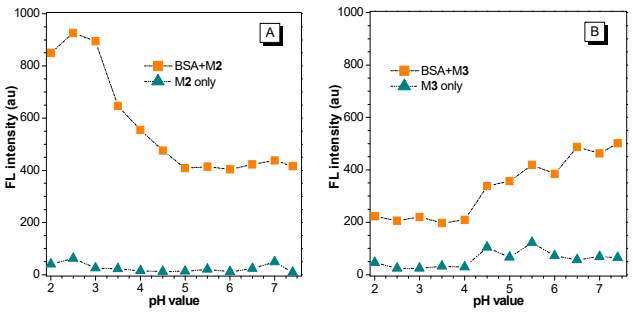

Figure 9. Variation of FL intensity of (A) M**2** and M**3** (B) in the presence or absence of BSA in PBS buffer with different pH values (2.0-7.4). λ_{ex}: 330 nm for M**2** and 395 nm for M**3**. Concentration of M**2** and M**3**: 1 μM; Concentration of BSA: 1 μM.

the two probes. The pH values of the two systems have been altered from 7.4 to 2.0, and the variation of the FL intensity recorded at the peak emission wavelength with pH are summarized in Figure 9 (see also Figures S13 and S14). Both M**2** and M**3** show neglectable FL intensity change in the pH range examined in the absence of BSA. For BSA+M**2** system, in the range of pH from 7.4 to 4.5, the FL intensity shows little change. When pH is reduced further to below 4.5, a gradual emission enhancement occurs and the intensity has been finally doubled at pH 2.0. When it comes to the system BSA+M**3**, along with pH altering from 7.4 to 2.0, the FL intensity undergoes a decrease until pH drops to about 4.5 and then levels off. The fluorescent behaviors of the two systems can be divided into two pH-relevant regions, and the breakpoint localizes at around the isoelectric point of BSA, which is approximate at 4.9.[33] When pH is lower than this point, the native BSA begins to isomerize to a partially-extended 'molten globule' state, which is predominantly populated at pH 3,[34] and the basic residues such as Arg and Lys are positively charged and repel the binding of positively charged M**3** but attract negatively charged M**2**. Consequently, below the breakpoint, the BSA+M**2** (Figure 9A) and BSA+M**3** (Figure 9B) systems display enhanced and weakened FL emission respectively.

Conclusions

In summary, the binding behaviours of BSA towards external species in its native, intermediate and unfolded states have been investigated by using two AIE-active fluorescent probes M**2** and M**3**, which are intentionally designed to bearing negative and positive charges respectively. On account of aggregation-induced emission property, M**2** and M**3** showed remarkably enhanced emissions as they binds to BSA. According to Stern-Volmer equation and FRET principle, it was estimated that BSA could bind to one probe M**2** or one M**3**, and the binding constant of M**2** and M**3** to native BSA was measured to be $5.50\times10^7$and 1.38×10^6 L/mol respectively. The displacement effects of site-specific binding ligands (myristic acid and warfarin) on the probes indicated that both of M**2** and M**3** selectively bound to the subdomain IIA of BSA. Hydrophobic interaction was the driving force of the binding process, regardless to the negative and positive charges carried by the probes.

When M**2** and M**3** were used to probe BSA unfolding process induced by thermal treating and by addition of denaturants urea or GndHCl, the differently charged probes showed drastically different fluorescent responses. As subdomain IIA rearranged and separated from other domains, its affinity to M**2** and M**3** evidently attenuates, for the hydrophobic pocket holding the probes was destroyed. When BSA went through a partial unfolding process responding to external stimuli, the buried pockets or cavities (Domain I) in BSA become a favourable site for specific binding of cationic M**3**, because the negatively charged residues exposed to the surroundings at this stage. In the cooling-induced refolding process, the formation of the hydrophobic pocket at Subdomain IIA accommodated both M**2** and M**3**, thus lighted up the emission from the probes. Meanwhile, the electrostatic interaction between cationic M**3** and the anionic residue in the unfolded Domain I allowed the excessive encapsulation of M**3** into the pocket of Domain I in the cooling run. Therefore, remarked enhancement emission form M**3** was recorded.

The experimental results reported herein are quite distinct from the data previously reported by fluorescent probes. In addition to hydrophobic interaction, by which BSA and other albumins to play its primary transport role, electrostatic interaction also plays crucial role in their responding towards charged species. The fluorescent behaviours of BSA towards the two ionic probes indicate M**2** and M**3** are efficient reporters of the folding, unfolding and refolding of BSA. Their emission changes disclose useful information about the loading and releasing of charged species, which will be instructive to the studies on pharmaceutics or drug pharmacokinetics.

Acknowledgements

This work was financially supported by the key project of the Ministry of Science and Technology of China (2013CB834704), the National Science Foundation of China (51573158), the Research Grants Council of Hong Kong (16301614, N_HKUST604/14 and N_HKUST620/11). J. Z. Sun thanks the financial support from Zhejiang Innovative Research Team Program (2013TD02). A. Qin and B. Z. Tang thank the support from Guangdong Innovative Research Team Program (201101C0105067115).

Notes and references

1 G. Fanali, A. di Masi, V. Trezza, M. Marino, M. Fasano, P. Ascenzi, *Mol. Aspects Med.* 2012, **33**, 209.
2 (a) F. Yang, Y. Zhang, H. Liang, *Int. J. Mol. Sci.* 2014, **15**, 3580; b) A. Varshney, P. Sen, E. Ahmad, M. Rehan, N. Subbarao, R. H. Khan, *Chirality* 2010, **2**2, 77; c) U. Kragh-Hansen, *Biochim. Biophys. Acta* 2013, **1830**, 5535.
3 (a) A. A. Bhattacharya, T. Grüne, S. Curry, *J. Mol. Biol.* 2000, **303**, 721; (b) I. Petitpas, T. Grüne, A. A. Bhattacharya, S. Curry, *J. Mol. Biol.* 2001, **314**, 955; (c) S. Curry, H. Mandelkow, P. Brick, N. Franks, *Nat. Struct. Biol.* 1998, **5**, 827.
4 (a) A. Ahmed-Ouameur, S. Diamantoglou, M. R. Sedaghat-Herati, S. Nafisi, R. Carpentier, H. A. Tajmir-Riahi, *Cell Biochem. Biophys.* 2006, **45**, 203; (b) S. Naveenraj, S. Anandan, *J. Photochem. Photobiol. C* 2013, **14**, 53.
5 (a) F. A. de Wolf, G. M. Brett, *Pharmacol. Rev.* 2000, **52**, 207; (b) F. Yang, C. Bian, L. Zhu, G. Zhao, Z. Huang, M. Huang, *J. Struct. Biol.* 2007, **157**, 348.
6 (a) A. Bujacz, *Acta Crystallogr. D Biol. Crystallogr.* 2012, **68**, 1278; (b) K. A. Majorek, P. J. Porebski, A. Dayal, M. D. Zimmerman, K. Jablonska, A. J. Stewart, M. Chruszcz, W. Minor, *Mol. Immunol.* 2012, **52**, 174.
7 (a) Y.-J. Hu, Y. Liu, L.-X. Zhang, R.-M. Zhao, S.-S. Qu, *J. Mol. Struct.* 2005, **750**, 174; (b) S. Shah, A. Sharma, M. N. Gupta, *Anal. Biochem.* 2006, **351**, 207; (c) L. Hu, S. Han, S. Parveen, Y. Yuan, L. Zhang, G. Xu, *Biosens. Bioelectron.* 2012, **32**, 297; (d) A. B. Kayitmazer, S. P. Strand, C. Tribet, W. Jaeger, P. L. Dubin, *Biomacromolecules* 2007, **8**, 3568; (e) C. M. Valmikinathan, S. Defroda, X. Yu, *Biomacromolecules* 2009, **10**, 1084.
8 U. Anand, S. Mukherjee, *Biochim. Biophys. Acta* 2013, **1830**, 5394.
9 (a) L. A. MacManus-Spencer, M. L. Tse, P. C. Hebert, H. N. Bischel, R. G. Luthy, *Anal. Chem.* 2010, **82**, 974; (b) C. Li, G. J.

Pielak, *J. Am. Chem. Soc.* 2009, **131**, 1368; (c) T. Wu, Q. Wu, S. Guan, H. Su, Z. Cai, *Biomacromolecules* 2007, **8**, 1899; (d) Q. Yang, J. Liang, H. Han, *J. Phys. Chem. B* 2009, **113**, 10454; (e) A. Valstar, M. Almgren, W. Brown, *Langmuir* 2000, **16**, 922.
10 (a) C. A. Royer, *Chem. Rev.* 2006, **106**, 1769; (b) F.-L. Cui, J.-L. Wang, Y.-R. Cui, J.-P. Li, *Anal. Chim. Acta* 2006, **571**, 175; (c) V. S. Jisha, K. T. Arun, M. Hariharan, D. Ramaiah, *J. Am. Chem. Soc.* 2006, **128**, 6024; (d) J. Jayabharathim, V. Thanikachalam, K. Saravanan, M. V. Perumal, *Spectrochim. Acta A* 2011, **79**, 1240.
11 (a) J. R. Lakowicz, J. Malicka, S. D'Auria, I. Gryczynski, *Anal. Biochem.* 2003, **320**, 13; (b) Y. Suzuki, K. Yokoyama, *J. Am. Chem. Soc.* 2005, **127**, 17799; (c) D. Ding, K. Li, B. Liu, B. Z. Tang, *Acc. Chem. Res.* 2013, **46**, 2441.
12 H. Tong, Y. Hong, Y. Dong, M. Häuβler, J. W. Y. Lam, Z. Li, Z. Guo, B. Z. Tang, *Chem. Commun.* 2006, 3705.
13 J. Mei, Y. Hong, J. W. Y. Lam, A. Qin, Y. Tang, B. Z. Tang, *Adv. Mater.* 2014, **26**, 5429.
14 H. Tong, Y. Hong, Y. Dong, M. Häuβler, Z. Li, J. W. Y. Lam, Y. Dong, H. H.-Y. Sung, I. D. Williams, B. Z. Tang, *J. Phys. Chem. B* 2007, **111**, 11817.
15 W. Z. Yuan, H. Zhao, X. Y. Shen, F. Mahtab, J. W. Y. Lam, J. Z. Sun, B. Z. Tang, *Macromolecules* 2009, **42**, 9400.
16 (a) X. Wang, J. Hu, G. Zhang, S. Liu, *J. Am. Chem. Soc.* 2014, **136**, 9890; (b) G. N. Zhao, B. Tang, Y. Q. Dong, W. H. Xie, B. Z. Tang, *J. Mater. Chem. B* 2014, **2**, 5093; (c) H. Shi, J. Liu, J. Geng, B. Z. Tang, B. Liu, *J. Am. Chem. Soc.* 2012, **134**, 9569; (d) Y. Hong, L. Meng, S. Chen, C. W. Tung, L.-T. Da, M. Faisal, D.-A. Silva, J. Liu, J. W. Y. Lam, X. Huang, B. Z. Tang, *J. Am. Chem. Soc.* 2012, **134**, 1680.
17 Y. Hong, C. Feng, Y. Yu, J. Liu, J. W. Y. Lam, K. Q. Luo, B. Z. Tang, *Anal. Chem.* 2010, **82**, 7035.
18 (a) J. K. Jin, X. J. Chen, Y. Liu, A. Qin, J. Z. Sun, B. Z. Tang, *Acta. Polym. Sin.* 2011, **9**, 1079; (b) T. Hu, X. J. Chen, B. C. Yao, A. Qin, J. Z. Sun, B. Z. Tang, *Chem. Commun.* 2015, **51**, 8849.
19 R. F. Chen, *J. Biol. Chem.*1967, **242**, 173.
20 (a) A. Sulkowska, *J. Mol. Struct.* 2002, **614**, 227; (b) Y. -Q. Wang, H. -M. Zhang, G. -C. Zhang, W. -H. Tao, S. -H. Tang, *J. Lumin.* 2007, **126**, 211.
21 (a) B. K. Paul, A. Samanta, N. Guchhait, *J. Phys. Chem. B* 2010, **114**, 6183; (b) N. Chadborn, J. Bryant, A. J. Bain, P. O'Shea, *Biophys. J.* 1999, **76**, 2198.
22 O. K. Abou-Zied, O. I. K. Al-Shihi, *J. Am. Chem. Soc.* 2008, **130**, 10793.
23 (a) S. Curry, P. Brick, N. P. Franks, *Biochim. Biophys. Acta* 1999, **1441**, 131; (b) D. P. Cistola, D. M. Small, J. A. Hamilton, *J. Biol. Chem.* 1987, **262**, 10980; (c) J. A. Hamilton, S. Era, S. P. Bhamidipati, R. G. Reed, *Proc. Natl. Acad. Sci. USA* 1991, **88**, 2051.
24 (a) G. Sudlow, D. J. Birkett, D. N. Wade, *Mol. Pharmacol.* 1975, **11**, 824; (b) G. Sudlow, D. J. Birkett, D. N. Wade, *Mol. Pharmacol.* 1976, **12**, 1052.
25 (a) L. Fu, S. Villette, S. Petoud, F. Fernandez-Alonso, M. Saboungi, *J. Phys. Chem. B* 2011, **115**, 1881; (b) G. Graziano, *Phys. Chem. Chem. Phys.* 2010, **12**, 14245.
26 Y. Moriyama, E. Watanabe, K. Kobayashi, H. Harano, E. Inui, K. Takeda, *J. Phys. Chem. B* 2008, **112**, 16585.
27 (a) D. Banerjee, S. K. Pal, *Photochem. Photobiol.* 2008, **84**, 750; (b) Y. Moriyama, Y. Kawasaka, K. Takeda, *J. Colloid Interface Sci.* 2003, **257**, 41; (c) C. Honda, H. Kamizono, T. Samejima, K. Endo, *Chem. Pharm. Bull.* 2000, **48**, 464.
28 (a) A. Chakrabarty, A. Mallick, B. Haldar, P. Das, N. Chattopadhyay, *Biomacromolecules* 2007, **8**, 920; (b) U. Kragh-Hansen, *Pharmacol. Rev.* 1981, **33**, 17.
29 (a) A. Chowdhury, V. Banerjee, R. Banerjee, K. P. Das, *Biopolymers* 2003, **101**, 549; (b) A. A. A. Halim, H. A. Kadir, S. Tayyab, *J. Biochem.* 2008, **144**, 33; (c) O. D. Monera, C. M. Kay, O. S. Hodges, *Protein. Sci.* 1994, **3**, 1984.
30 (a) W. K. Lima, J. Rösgen, S. W. Englandera, *Proc. Natl. Acad. Sci. USA* 2009, **106**, 2595; (b) R. Kumaran, P. Ramamurthy, *J. Fluoresc.* 2011, **21**, 1499.
31 (a) U. Anand, C. Jash, S. Mukherjee, *Phys. Chem. Chem. Phys.* 2011, **13**, 20418; (b) B. Ahmad, M. Z. Ahmed, S. K. Haq, R. H. Khan, *Biochim. Biophys. Acta* 2005, **1750**, 93.
32 (a) S. Tayyab, N. Sharma, M. M. Khan, *Biochem. Biophys. Res. Commun.* 2000, **277**, 83; (b) M. Y. Khan, S. K. Agarwal, S. Hangloo, *J. Biochem.* 1987, **102**, 313; (c) N. Ahmad, M. A. Qasim, *Eur. J. Biochem.* 1995, **227**, 563.
33 Y. Li, J. Lee, J. Lai, L. An, Q. Huang, *J. Phys. Chem. B* 2008, **112**, 3797.
34 M. Bhattacharya, N. Jain, K. Bhasne, V. Kumari, S. Mukhopadhyay, *J. Fluoresc.* 2011, **21**, 1083.